scientific reports

Check for updates

OPEN

Genome-wide identification and expression analysis of *ACS* and *ACO* gene family in *Ziziphus jujuba* mill during fruit ripening

Zhuo Chen[1,2], Gang Jin[3], Zhaokun Zhi[2], Yanmeng Guo[2], Yiteng Liu[1], Bingxin Fan[1], Gao-Pu Zhu[1,2]✉, Mengmeng Zhang[1]✉ & Shulin Zhang[1,2]✉

The jujube (*Ziziphus jujuba* Mill.) cultivar 'Dongzao' is globally popular as a fresh fruit but faces challenges with shelf life, which is positively associated with ethylene production. The two key enzymes involved in ethylene biosynthesis, 1-Aminocyclopropane-1-Carboxylic acid Synthase (ACS) and 1-Aminocyclopropane-1-Carboxylic acid Oxidase (ACO), are encoded by *ACS* and *ACO* gene families, respectively. This study identified 7 *ZjACS* genes and 36 *ZjACO* genes in 'Dongzao' and revealed extensive evolutionary divergence between 'Dongzao' and *Arabidopsis thaliana*. Phylogenetic relationships were more apparent when analyzing genes with similar structures, motifs and subcellular localization predictions. Transcriptome profiling showed that a substantial number of the *ZjACS* and *ZjACO* genes displayed stage-specific expression tendency during fruit development. Co-expression analysis showed that 4 *ZjACS* and 9 *ZjACO* genes were linked to transcription factors (TFs) involved in fruit ripening. The diverse regulatory factors, including ERF, NAC and WRKY TFs and *cis*-acting regulatory elements, likely contribute to the complex roles of the *ZjACSs* and *ZjACOs* during ripening of jujube fruits. This study sheds light on the genetic regulation of ethylene biosynthesis in 'Dongzao' jujube ripening, providing insights for postharvest research in this economically important species.

Keywords Jujube (*Ziziphus Jujuba* Mill), Ethylene biosynthesis, ACS, ACO, Genome-wide analysis

Plant growth and development relies on complex phytohormonal regulatory networks that include ethylene[1,2], jasmonic acid[3,4], cytokinins[5], gibberellins[6], abscisic acid[7,8], and brassinosteroids (BRs)[9]. Ethylene, a gaseous phytohormone, governs seed dormancy, organ development, stress responses, and notably fruit ripening. Ethylene also serves as a crucial mediator between external environmental changes and internal plant developmental responses[10–12]. In climacteric fruits, ripening involves synchronized ethylene production spikes and respiratory bursts, directly controlling sugar accumulation, color change and texture modification[13]. Intriguingly, previous studies found that ethylene plays an important role in controlling ripening of non-climacteric fruit (like jujube), which maintain low ethylene content[14–17]. Comprehending the molecular mechanisms driving ethylene biosynthesis and its regulation is crucial for deciphering the orchestration of fruit maturation.

The ethylene biosynthesis pathway requires two committed enzymatic reactions. In the first progress, S-adenosyl-L-methionine (SAM) is converted to ACC and 5'-methylthioadenosine (MTA) by the enzyme ACS. In the second, ACC is converted to ethylene, CO_2 and cyanide by the enzyme ACO[18]. These rate-limiting enzymes are evolutionarily conserved across plants, with gene family expansions reflecting functional specialization. In plants, the coding genes and the functions of ACS and ACO enzymes have been extensively investigated[18,19]. In *Arabidopsis thaliana*, there are 10 *AtACSs* and 5 *AtACOs*, and nine of the AtACS (AtACS1, AtACS2, AtACS4-9, and AtACS11) exhibit catalytic functions, only *AtACS3* functions as a pseudogene, while AtACS10 and AtACS12 exhibit aminotransferase activity. These AtACS proteins are divided into 3 types based on which interaction domains are in their sequences. Type 1 AtACS proteins have target sites for mitogen-activated and calcium-dependent protein kinases (MAPKs and CDPKs, found in AtACS1, AtACS2, and AtACS6, respectively), Type 2 AtACS (AtACS4, AtACS5, AtACS8, AtACS9, and AtACS11) are targets for CDPKs and E3 ligases, and the Type

[1]Research Institute of Non-Timber Forestry, Chinese Academy of Forestry, Zhengzhou 450003, China. [2]School of Horticulture and Landscape Architecture, Henan Institute of Science and Technology, Xinxiang 453003, China. [3]Guangxi Key Laboratory of Quality and Safety Control for Subtropical Fruits, Guangxi Subtropical Crops Research Institute, Nanning 530001, China. ✉email: poog502@hotmail.com; mmz19930409@163.com; shulinzhng@gmail.com

3 AtACS contains no known target sites (AtACS7)[20]. Likewise, the AtACO protein family can be divided into three types based on amino acid sequence similarity of the conserved dioxygenase-specific RXS motif: Type 1 (AtACO2, AtACO3, AtACO4), Type 2 (AtACO1), and Type 3 (AtACO5)[21]. In tomato, there are 14 *SlACS* genes and 6 *SlACO* genes. *SlACS2*, *SlACS4*, *SlACO1* and *SlACO4* showed distinct expression patterns during fruit ripening and are the main *SlACS* and *SlACO* supporting ripening-associated ethylene production[22]. In strawberry, 5 *FaACSs* and 4 *FaACOs* were identified and showed different expression tendencies during fruit ripening[23]. In pear, 11 *PuACSs* and 8 *PuACOs* were expressed during different stages of ripening, and 4 *PuACSs* and 3 *PuACOs* genes could be induced by ethephon and inhibited by 1-MCP treatment[24].

Additionally, diverse regulatory mechanisms have been extensively documented for the roles that ACSs and ACOs play in fruit maturation. Several studies have revealed that the expression of *ACO* and *ACS* was regulated by multiple TFs, including Ethylene Response Factor (ERF), NAM/ATAF/CUC2 (NAC), and WRKY. In apple, MdERF2 negatively regulates the synthesis of ethylene and the fruits ripening by inhibiting the transcription of *MdACS1*[25]. Furthermore, the TFs MdERF008 and MdNAC71 bound to the promoter region of *MdACS1* and directly control its transcription, thereby controlling ethylene biosynthesis in apple fruits[26]. In tomato, SlNAC4 and SlNAC9 bind with *LeACS2*, *LeACS4*, and *LeACO1* promoters, affecting ripening of tomato fruits[27]. In kiwifruit, AcWRKY4 is involved in postharvest kiwi ripening by binding to the promoters of *AcACS1* and *AcACS2* to activate their expression[28]. Despite these advances in climacteric fruits, functional studies remain scarce for non-climacteric species beyond basic expression profiling in strawberry[29], sand pear[30], and grape[31], highlighting a critical knowledge gap in ethylene regulation diversity.

The fresh jujube cultivar 'Dongzao' is appreciated by consumers for its flavor, crispness, and nutritional value, and is cultivated worldwide for its economic value[32,33]. However, postharvest fresh jujube fruits exhibit high respiration rates and rapid water loss, resulting in a very short shelf life. When stored at ambient temperatures, shelf life remains marketable for only 3–5 days, severely limiting their transport and market reach[34]. Therefore, elucidating the regulatory mechanisms underlying jujube fruit ripening is critical for extending postharvest storage, enhancing fruit quality, optimizing harvest timing, and advancing varietal improvement to boost economic benefits. The role of ethylene in regulating non-climacteric fruit ripening has long been debated. However, emerging studies suggest that ethylene, despite maintaining low levels, plays a significant regulatory role in the maturation of non-climacteric fruits[14–17]. As a non-climacteric fruit, the *ZjACS* and *ZjACO* gene families, key enzymes for ethylene synthesis in 'Dongzao' jujube, have not been adequately explored, resulting in a restricted comprehension of the *ZjACS* and *ZjACO* gene families. To minimize this comprehension gap, we first performed a genome-wide analysis to identify the *ZjACS* and *ZjACO* genes in 'Dongzao'. Then we extensively investigated the evolutionary relationships, gene structures, conserved motifs, collinearity relationships, and *cis*-regulatory elements of the *ZjACS* and *ZjACO* genes. Additionally, we investigated their expression profiles and co-expression networks with various fruit ripening-associated transcription factors during fruit maturation. Our findings provide light on the rich variety of the *ZjACS* and *ZjACO* gene families, as well as their possible functions in ethylene biosynthesis and fruit maturation in jujube.

Materials and methods

Plant materials

Fruits were sampled from healthy, 10-year-old jujube trees of the cultivar 'Dongzao' in Anyang City, Henan Province, China (geographical location: 34°51′35′′ N, 112°42′51′′ E) at 40, 55, 70, 85, 100, 115 and 130 days after pollination (DAP). The seven sampling time points were between mid-July and the end of October in 2023, and named as S1, S2, S3, S4, S5, S6 and S7. At each stage, twenty fruits were mixed as one biological replicate, and each stage had three replicates. After removing the seed, sampls were quickly frozen in liquid nitrogen and kept at -80 °C for extracting RNA.

Extraction and determination of *ACS* and *ACO* activities

The activities of ACS and ACO enyzemes in jujube were assessed using ELISA detection kits for Plant ACC Synthase (ACS) and Plant ACC Oxidase (ACO) from Shanghai Enzyme-linked Biotechnology Co., Ltd. (mlbio, Shanghai, China). Fresh jujube samples from different stages (– 100 mg) were crushed in liquid nitrogen before being transferred to a 2-mL centrifuge tube, kept on ice, and mized with 0.9 mL of homogenizing solution (PBS, pH 7.4, 0.01 mol/L). The mixture was centrifuged at 8000 g for 15 min. The supernatant was collected for analysis.

Identification of *ACS* and *ACO* genes in 'Dongzao' genome

To identify the ACS and ACO proteins from three *Ziziphus jujuba* cultivars, 'Dongzao', 'Suanzao' and 'Junzao', the newest jujube genomes with gene annotation were acquired from NCBI (https://www.ncbi.nlm.nih.gov/) by a global search[35]. Phytozome (http://phytozome.jgi.doe.gov/pz/portal.html) provided the ACS and ACO protein sequences for Arabidopsis, *Fragaria* × *ananassa*, *Malus* × *domestica*, and *Solanum lycopersicum*. The protein basic local alignment search tool (BLASTp) was used to search for these sequences, with a threshold E-value of 10^{-10}. Furthermore, HMM profiles were created utilizing conserved ACS and ACO domain sequences derived from ACS (PF00155) and ACO (PF14226, PF03171)[36]. The putative jujube ACS and ACO proteins in jujube were found through HMM profiles and HMMER software (version 3.0) utilizing a standard E-value. Redundant sequences were removed to guarantee that the unique *ACS* and *ACO* genes. Calculation of the molecular weights and the isoelectric points (PIs) for the presumed jujube ACS and ACO proteins utilized ExPASy (http://web.expasy.org/compute_pi/). Furthermore, the WoLF PSORT site (https://wolfpsort.hgc.jp/) served the purpose of forecasting subcellular positioning.

Phylogenetic analysis
The phylogenetic tree of the ACO and ACS proteins was built with the Neighbor-Joining (NJ) technique and a bootstrap value of 1000 in MEGA version 11.0 and was visualized using Evolview 3.0 (https://evolgenius.info//evolview-v2).

Analysis of predicted *ACS* and *ACO* genes from 'Dongzao' jujube
The exons/introns of the *ZjACS* and *ZjACO* genes were determined using the Gene Structure Display Server (GSDS2.0: https://gsds.gao-lab.org/Gsds_help.php) based on the coding and corresponding genomic sequences[37].

Conserved motifs within the predicted ZjACS and ZjACO proteins were determined through the online tool Motif Elicitation (MEME) version 5.5.7 (https://meme-suite.org/meme/)[38], adhering to these criteria: (1) motif occurrences were restricted to 0 or 1 per sequence; (2) a maximum of 10 motifs were considered; (3) the optimum motif width was set between 6 and 50 amino acids; and (4) only motifs with an E-value below 0.05 were considered significant[39].

The upstream promoter regions (2000 bp) of each *ACS* and *ACO* genes from 'Dongzao' genome were extracted with TBtools software and upload to PlantCARE (https://bioinformatics.psb.ugent.be/webtools/plantcare/html/), which could examine the *cis*-regulatory elements[40]. Classification of the cis-acting elements was determined by their predicted function.

Chromosomal distribution and gene duplication analysis
Chromosomal locations of the *ZjACS*s and *ZjACOs* were obtained from the annotation information of the 'Dongzao' genome database and analyzed through the Gene Location Visualization feature of TBtools[41]. For illustrating the synteny of the orthologous *ACS* and *ACO* genes founded in 'Dongzao' and other chosen genomes, we examined gene duplication occurrences using the Multicollinearity Scanning Toolkit (MCScanX)[42] with its standard settings, and then employed the Circos and Dual Synteny Plot results in TBtools. Calculations for the evolutionary rates *Ka*, *Ks*, and the *Ka/Ks* ratio calculated in KaKs_Calculator 3.0[17,43].

Expression profiles analysis based on RNA-seq data
Transcriptome sequencing data from seven samples (*Z. jujuba* 'Dongzao', at 40, 55, 70, 85,100, 115 and 130 days after pollination), were generated (SMART BIOTECH, Illumina HiSeq 4000) and deposited in NCBI (PRJNA1173509). The raw data were individually aligned with the jujube genome (NCBI, ASM3175591v1) via HISAT2 v2.0.5 using standard settings[44], and gene expression was ascertained through the fragment count per kilobase per million mapped exons (FPKM) technique. Genes exhibiting differential expression were additionally pinpointed through the DESeq2 R package in R (version 1.16.1), ensuring $p < 0.05$ and absolute $\log_2$ (fold change) values exceeded 1[45]. Ultimately, heatmaps were created by TBtools[41].

Co-expression network analysis
Based on the transcriptome and qRT-PCR datasets, the Pearson's correlation coefficients (PC) were calculated between two genes through R package. Genes with expression correlation coefficients greater than 0.9 were identified as co-expressed. Co-expression between *ACS* and *ACO* genes and fruit ripening related transcription factors were analyzed and a co-expression network was created and shown using Cytoscape v.3.7.1[46].

qRT-PCR analysis of *ZjACSs* and *ZjACOs*
Total RNA extraction was performed using a plant RNA extraction kit (Vazyme, Nanjing, China). Utilizing a HiScript II Q RT SuperMix for qPCR (+gDNA wiper) (R223-01, Vazyme, Nanjing, China), the initial strand of cDNA was produced as 1000 ng of total RNA. In addition, qRT-PCR was done utilizing a ChamQ Universal SYBR qPCR Master Mix (Q711-02, Vazyme, Nanjing, China), totaling 20 µL, including 2.0 µL cDNA, 10 µL SYBR premix solution, 0.4 µL forward/reverse primers and 7.2 µL ddH_2O. The procedure for the PCR thermal program was established in this manner: 95 °C for 60s, then 40 cycles of amplification for 10s at 95 °C, 30 s at 59 °C, and a standard dissociation phase in a Bio-Rad CFX Connect system. The $2^{-\Delta\Delta CT}$ method was employed to calculate the comparative expression levels of the *ZjACSs* and *ZjACOs*[47], with t-tests applied for statistical evaluation. The primers used for the qRT-PCR analysis are listed in Table S6.

Statistical analysis
All data are the average of three duplicates. GraphPad software version 10.0 was used to statistical analysis. The student's t-test and one-way ANOVA were employed to assess the variances at a significance level of $p < 0.05$.

Results
Ethylene biosynthesis enzyme activity during jujube fruit development
Numerous studies have showed that ethylene is essential to the growth and maturity of jujube fruit and that the activities of ACC synthase (ACS) and ACC oxidase (ACO) restrict the production of ethylene[18,21,48]. 'Dongzao' fruit samples were collected 40, 55, 70, 85, 100, 115, and 130 days after pollination (DAP, named as S1, S2, S3, S4, S5, S6, and S7), and the ACS and ACO activities were examined (Fig. 1). There is an increasing trend in ACS activity throughout jujube fruit development. In contrast, ACO activity increased from S1 to S4, followed by a slight decline from S5 to S6, and then another increase from S6 to S7. These results revealed the likely roles of ACS and ACO in 'Dongzao' fruit development.

Identification and characterization of *ACS* and *ACO* genes in 'Dongzao' jujube genome
To clarify the function of ACS and ACO enzymes in 'Dongzao', the *ACS* and *ACO* genes were identified through a genome-wide analysis. A total of 7 *ACS* genes and 36 *ACO* genes were identified in the 'Dongzao' genome

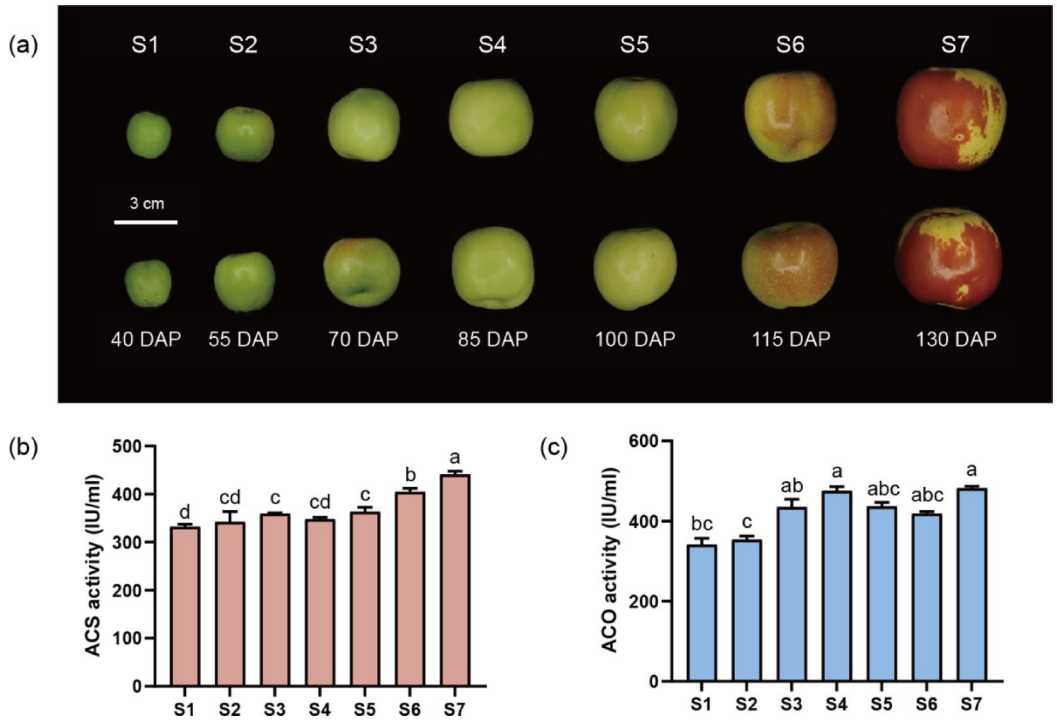

Fig. 1. Changes in fruit phenotype and activities of ACC synthase (ACS) and ACC oxidase (ACO) enzymes during the ripening of 'Dongzao' jujube. (**a**) Phenotype of 'Dongzao' jujube at different developmental stages. Scale bar, 3 cm. (**b**, **c**) ACS and ACO enzymes activity analysis. Variations in letters signify statistically notable disparities at various phases, as determined by one-way ANOVA ($P < 0.05$). The standard deviation of the duplicates is denoted by the error bars.

(Fig. 2, Table S1). Comparing the *ACS* and *ACO* genes across various plant species, there are fewer *ACS* genes predicted in jujube compared with Arabidopsis, while there are significantly more *ACO* genes (Fig. 2a). The physicochemical properties of the ACS and ACO proteins were predicted (Fig. 2b), showing that the 7 *ACS* genes encoded proteins ranging from 470 (ZjACS5) to 561 (ZjACS7) amino acids in length, and 52,407.22 Da (ZjACS5) to 60,554.1 Da (ZjACS7) in size. The proteins encoded by the 36 *ACO* genes were predicted to contain between 216 (ZjACO31) and 416 (ZjACO29) amino acids, with molecular weights (MWs) varying between 24,822.25 Da (ZjACO31) and 48,037.36 Da (ZjACO29). The ACS and ACO proteins were predicted to have high aliphatic amino acid index (AI) values, with thermal stability values for ACS ranging from 78.96 (ZjACS4) to 96.33 (ZjACS6) and for ACO ranging from 77.45 (ZjACO6) to 97.94 (ZjACO22). Prediction of subcellular localization indicated that ACS proteins would primarily be found in the chloroplast, with a few (ZjACS2 and ZjACS4) localized in cytoplasm, while all ACO proteins were expected to be located in the cytoplasm. The variety of subcellular localization indicates different biological roles for 'Dongzao' jujube *ACS* and *ACO* gene families[49].

Phylogenetic analysis of 'Dongzao' *ACS* and *ACO* genes

To explore the evolutionary relationships of the *ACS* and *ACO* gene families between three jujube cultivars ('Dongzao', 'Junzao', 'Suanzao'), with sequences from Arabidopsis as an outlier, phylogenetic trees were constructed (Fig. 3). As seen in the phylogenetic trees, the *ACS* genes could be divided into four subtypes (Fig. 3a). Types I, II, and IV each contained 2 *ZjACS* genes, while there was one *ACO* gene in type III, from 'Dongzao'. Furthermore, the type IV genes were grouped with the greatest bootstrap values, followed by type III.

The ACO proteins could be classified into three major types, with the type III genes further subdivided into four subtypes (Fig. 3b). Among the major types, type I contained genes only from 'Dongzao' jujube, suggesting that these genes might be unique to 'Dongzao'. In contrast, the classes II and III-4 did not contain any sequences from 'Dongzao' jujube, while the other types included genes from all three jujube cultivars and Arabidopsis. In subclasses III-2 and III-3, each jujube cultivar has the same number of genes as its corresponding subfamily in Arabidopsis (1 ZjACO, 1 JzACO, 1 SzACO and 1 AtACO), while the number of type III-1 in Arabidopsis was 1.5 times that in each jujube cultivar (2 ZjACOs, 2 JzACOs, 2 SzACOs and 3 AtACOs).

Gene structure and conserved motif analyses of the *ZjACS* and *ZjACO* family genes in 'Dongzao'

The exon and intron structures as well as the diversity of motifs in a sequence, can provide insights into the evolution of family members. Therefore, the gene structures and conserved motifs of the *ACS* and *ACO* gene families in 'Dongzao' jujube were analyzed combination with their phylogenetic relationships (Fig. 4). In ZjACS

(a)

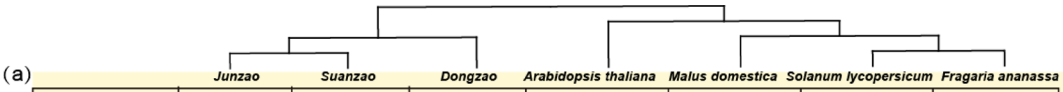

Genomic version	ASM3711355v1	ASM3711354v1	ASM3175591v1	Tair10	v1.0	v2.0	v1.0
Chromosome number	12	12	12	7	17	12	14
Gene name prefix	Jz	Sz	Zj	At	Md	Sl	Fa
ACS genes	8	8	7	12	20	23	26
ACO genes	24	26	36	5	31	32	76

(b)

Gene Family	Gene Name	Protein ID	Gene ID	Chromosome	Gene Length (bp)	Protein Length (aa)	MW(Da)	pI	A.I.	GRAVY	Stability	Predicted Location
ACS	*ZjACS1*	XP_048320486.1	107430205	NC_083384.1	2095	478	53784.46	5.99	85.84	-0.222	U	Chloroplast.
	ZjACS2	XP_015885091.3	107420607	NC_083383.1	1543	471	52602.42	9	83.61	-0.241	S	Cytoplasm.
	ZjACS3	XP_015899652.2	107432945	NC_083389.1	2110	500	56171.99	6.65	79.72	-0.269	U	Chloroplast
	ZjACS4	XP_048334674.2	107425000	NC_083385.1	2422	473	53622.15	8.67	78.96	-0.332	U	Cytoplasm
	ZjACS5	XP_015889144.3	107423985	NC_083385.1	1934	470	52407.22	5.7	84.47	-0.235	U	Chloroplast
	ZjACS6	XP_015877869.3	107414271	NC_083386.1	1745	507	55845.1	7.52	96.33	-0.053	U	Chloroplast
	ZjACS7	XP_015901591.2	107434621	NC_083384.1	1920	561	60554.1	8.44	88.45	-0.13	U	Chloroplast
ACO	*ZjACO1*	NP_001310797.1	107417150	NC_083382.1	1097	319	36243.73	5.65	83.13	-0.379	S	Cytoplasm
	ZjACO2	XP_015887933.3	107422939	NC_083381.1	1483	378	42668.63	5.14	87.65	-0.296	S	Cytoplasm
	ZjACO3	XP_015887930.3	107422935	NC_083381.1	1348	358	40455.16	5.67	84.39	-0.337	U	Cytoplasm
	ZjACO4	XP_048333201.2	107422936	NC_083381.1	1679	375	42374.9	5.46	90.67	-0.334	S	Cytoplasm
	ZjACO5	XP_048333196.2	125423377	NC_083381.1	1313	379	43323.23	5.41	78.87	-0.425	S	Cytoplasm
	ZjACO6	XP_015889118.2	107423970	NC_083385.1	1507	325	37404.6	7.26	77.45	-0.574	U	Cytoplasm
	ZjACO7	XP_015891482.1	107425928	NC_083387.1	2276	373	42394.2	6.2	81.47	-0.415	U	Cytoplasm
	ZjACO8	XP_048333192.2	107422929	NC_083381.1	1535	378	42771.66	5.52	92.25	-0.28	S	Cytoplasm
	ZjACO9	XP_060671781.1	132803250	NC_083381.1	1581	375	42275.15	5.77	83.65	-0.407	S	Cytoplasm
	ZjACO10	XP_015887932.2	107422938	NC_083381.1	1585	375	42275.15	5.77	83.65	-0.407	S	Cytoplasm
	ZjACO11	XP_015895397.1	107429258	NC_083390.1	1463	368	41054.39	5.27	83.89	-0.413	S	Cytoplasm
	ZjACO12	XP_060671607.1	107422934	NC_083381.1	1711	332	37509.17	5.44	95.36	-0.123	U	Cytoplasm
	ZjACO13	XP_015898632.1	107432086	NC_083389.1	1871	368	40876.42	5.59	84.73	-0.295	S	Cytoplasm
	ZjACO14	XP_048333190.2	125423375	NC_083381.1	1528	380	43020.86	5.79	83.32	-0.413	S	Cytoplasm
	ZjACO15	XP_060671605.1	107422915	NC_083381.1	1720	380	43133.09	5.18	85.39	-0.346	S	Cytoplasm
	ZjACO16	XP_048333193.2	107422925	NC_083381.1	1309	380	42901.8	5.31	88.47	-0.327	S	Cytoplasm
	ZjACO17	XP_048333218.2	125423391	NC_083381.1	1571	378	42680.45	5.5	85.56	-0.406	S	Cytoplasm
	ZjACO18	XP_060669298.1	125418408	NC_083390.1	2554	395	44653.12	5.68	88	-0.322	S	Cytoplasm
	ZjACO19	XP_060672013.1	107422819	NC_083381.1	1326	372	41905.6	5.46	86.69	-0.373	S	Cytoplasm
	ZjACO20	NP_001310795.1	107414763	NC_083379.1	1097	321	36515.98	5.2	83.24	-0.373	S	Cytoplasm
	ZjACO21	XP_015887934.3	107422940	NC_083381.1	1617	373	42237.14	5.55	92.98	-0.305	S	Cytoplasm
	ZjACO22	XP_015887935.2	107422943	NC_083381.1	1122	373	42080.04	5.89	97.94	-0.216	S	Cytoplasm
	ZjACO23	XP_015887925.3	107422930	NC_083381.1	1238	372	41565.25	5.48	96.64	-0.241	S	Cytoplasm
	ZjACO24	XP_015887942.3	107422951	NC_083381.1	1502	378	42719.65	5.32	89.71	-0.312	S	Cytoplasm
	ZjACO25	XP_048333199.1	125423379	NC_083381.1	1521	378	42669.59	5.38	90.21	-0.308	S	Cytoplasm
	ZjACO26	XP_048332878.2	107422923	NC_083381.1	1529	392	44612.48	5.77	78.04	-0.417	S	Cytoplasm
	ZjACO27	XP_048333219.2	125423392	NC_083381.1	1554	391	44411.58	5.97	83.99	-0.343	U	Cytoplasm
	ZjACO28	XP_048331963.1	107421119	NC_083383.1	1407	312	35372.11	5.31	80.29	-0.466	S	Cytoplasm
	ZjACO29	XP_048326828.1	107403401	NC_083386.1	1251	416	48037.36	6.24	81.08	-0.573	U	Cytoplasm
	ZjACO30	XP_048326831.1	125421634	NC_083386.1	1422	372	42403.05	5.5	83.06	-0.438	S	Cytoplasm
	ZjACO31	XP_048326832.1	107435816	NC_083386.1	651	216	24822.25	5.89	83.89	-0.523	S	Cytoplasm
	ZjACO32	XP_060668147.1	107412297	NC_083388.1	657	218	25331.51	6.4	88.49	-0.137	U	Cytoplasm
	ZjACO33	XP_015887926.3	107422932	NC_083381.1	1583	375	42238.73	5.31	91.41	-0.327	S	Cytoplasm
	ZjACO34	XP_015875530.2	107412300	NC_083388.1	1684	371	41760.89	5.87	86.47	-0.293	U	Cytoplasm
	ZjACO35	XP_015887927.3	107422933	NC_083381.1	1511	380	43232.25	5.66	86.42	-0.384	S	Cytoplasm
	ZjACO36	XP_048333187.2	107422928	NC_083381.1	1522	381	43198.6	6.25	88.22	-0.382	S	Cytoplasm

Fig. 2. Identification and physicochemical properties of *ZjACSs* and *ZjACOs* genes in 'Dongzao' jujube. (**a**) The number of *ACS* and *ACO* genes identified in the *Ziziphus jujuba*, *Arabidopsis thaliana*, *Malus* × *domestica*, *Solanum lycopersicum*, and *Fragaria* × *ananassa* genomes. (**b**) Predicted physicochemical properties of ACS and ACO proteins in 'Dongzao' jujube.

proteins, motif composition and exon/intron structures exhibited a consistent pattern within a subfamily, while different subfamilies displayed markedly divergent structures (Fig. 4a). The count of preserved motifs varied between 9 and 10, exhibiting variations in their composition (Fig. 4b; Table S2). Among them, ZjACS7 did not contain motif 9, while all other ZjACSs contained motif 1–10. The exon/intron structures revealed that 7 *ZjACS* genes contained introns, of which 6 contained three introns, 1 (*ZjACS5*) contained one intron (Fig. 4c). For ZjACO proteins, proteins with similar motif distributions and gene structure were clustered (Fig. 4d). All ZjACO proteins contained four of the motifs (motifs 1, 2, 7 and 9). Motifs 3, 5, 6, and 10 were only found in type I ACOs, whereas motifs 4 and 8 were present in all ZjACO proteins except for ZjACO4 and ZjACO8. ZjACO proteins in class I had different conserved motif compositions, whereas type III-1, III-2, and III-3 ZjACO proteins shared the same conserved motif composition, suggesting that some of the family members exhibited high conservation while others had notable variation (Fig. 4e). All 36 *ZjACO* genes contained exons and introns, and that 32 *ZjACO* genes contained UTRs, except *ZjACO22*, *ZjACO29*, *ZjACO31*, *ZjACO32*. All type I *ZjACO* genes had no more

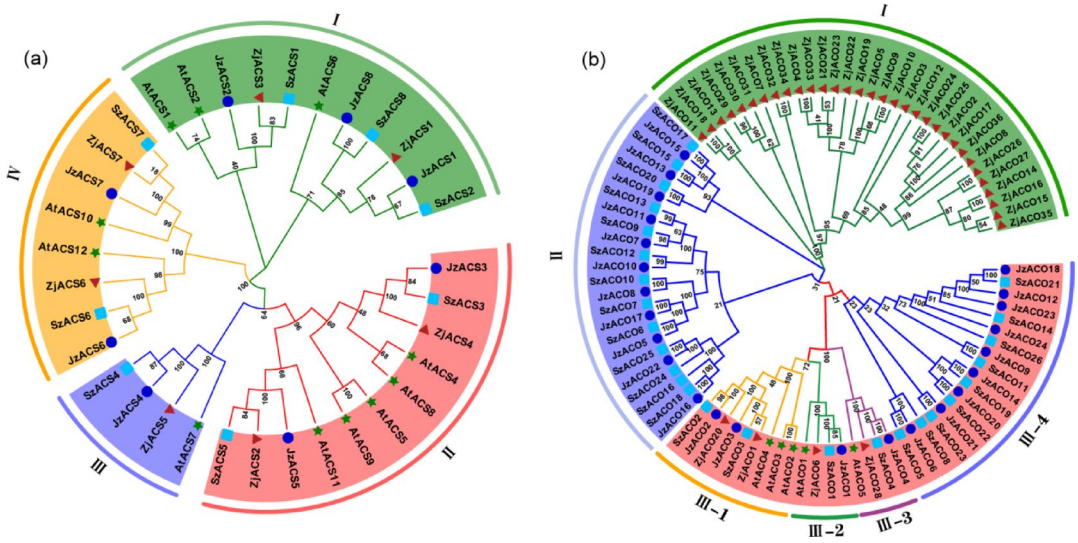

Fig. 3. Phylogenetic trees of *ACS* and *ACO* family genes. (**a**) *ACS* genes from three jujube cultivars ('Dongzao' ▲, 'Junzao' ●, 'Suanzao' ▪) and Arabidopsis (★). (**b**) *ACO* genes from three jujube cultivars and Arabidopsis. Using neighbor-joining (NJ) with 1000 bootstrap replicates, the tree's construction was executed in MEGA 11 software. Gene family members from 'Dongzao', 'Junzao', 'Suanzao', and Arabidopsis are denoted by a red triangle, a blue circle, a teal square, and a green star, respectively. Branches of varying colors symbolize diverse gene subfamilies.

than three introns, except for *ZjACO31* and *ZjACO29*, while both type III-1 members contained three introns (Fig. 4f).

Promoter region *cis*-acting regulatory elements

To predict the regulatory behavior of different *ZjACS* and *ZjACO* genes in 'Dongzao' jujube, the *cis*-acting regulatory elements (CREs) within the 2-kb promoter regions of the *ZjACS* and *ZjACO* genes were analyzed (Table S3). A variety of CREs related to phytohormones were found in the upstream sequences (Fig. 5). Response elements related to six types of hormones, namely ETH, ABA, MeJA, gibberellin, auxin, and salicylic acid, were found.

In the promoter regions of the *ZjACS* genes (Fig. 5b and c), all seven *ZjACS* genes contained CREs associated with ABA, MeJA, ETH, salicylic acid, gibberellin, and auxin responsiveness, indicating that ZjACS proteins were likely subject to regulation by various hormone signals. We also noticed that *ZjACS2* contained the largest number of *cis*-elements related to hormones.

ZjACOs gene promoters were particularly enriched with ABA-responsive elements (ABRE) and MeJA-responsive elements (CGTCA-motif and TGACG-motif) (Fig. 5e and f). Specifically, CREs associated with abscisic acid response were present in 27 out of 36 *ZjACOs* across all subfamilies. MeJA-responsive CREs were predominantly observed in certain subfamilies, while approximately 75% of all *ZjACOs* (20 out of 36), particularly in subfamilies I, III-1, and III-2, contained auxin-responsive CREs (CGTCA-motif and TGACG-motif) in their promoter regions. Additionally, 8 of the 36 *ZjACOs*, namely *ZjACO1*, *ZjACO2*, *ZjACO7*, *ZjACO13*, *ZjACO18*, *ZjACO22*, *ZjACO28*, and *ZjACO34*, contained ethylene-responsive CREs (DRE1 and DRE core) in their promoter regions. Furthermore, several *ZjACOs* promoter regions contained multiple elements that respond to the same hormone, indicating the potential for more rapid and intense hormonal responses. Conversely, some *ZjACOs*, such as *ZjACO13*, *ZjACO23*, *ZjACO28*, and *ZjACO31*, contained diverse hormone response elements, indicating their possible involvement in multiple regulatory networks.

Chromosomal location and collinearity analysis of *ZjACS* and *ZjACO* genes

To study locus relationships among the *ZjACS* and *ZjACO* genes in jujube, the distribution and collinearity of the *ZjACS* and *ZjACO* genes in the 'Dongzao' genome were analyzed. The 7 *ZjACS* genes and 36 *ZjACO* genes were unequally distributed on twelve jujube linkage groups (Fig. 6a). The largest number of *ZjACS* genes occurred on NC_083384.1 (2 *ACS* genes), and all 7 *ZiACS* genes were segmentally duplicated genes. The largest number of *ZjACO* genes occurred on NC_083381.1 (23 *ACO* genes), implying that this location may have significantly influence on the expansion of the relatively large *ZjACO* gene family in 'Dongzao'. Among the 36 *ACO* genes, 30 *ZjACO* genes were derived from tandem duplication in 'Dongzao' jujube, while the remaining 6 *ZjACO* genes were derived from segmental duplication. The MCScanX approach was utilized to further evaluate the gene duplication events in the 'Dongzao' genome, and uncover 5 gene pairs presumably originated from gene duplication events were found (Fig. 6a). These results suggested that these *ACS* and *ACO* genes may have arisen through gene duplication. The *Ka/Ks* ratio, which compares the amounts of nonsynonymous substitutions at each nonsynonymous site (*Ka*) with the total synonymous substitutions at each synonymous site (*Ks*), was determined for all five duplicated gene pairs (Table S4). Merely one pair (*ZjACO20- ZjACO1*) exhibited a *Ka/Ks*

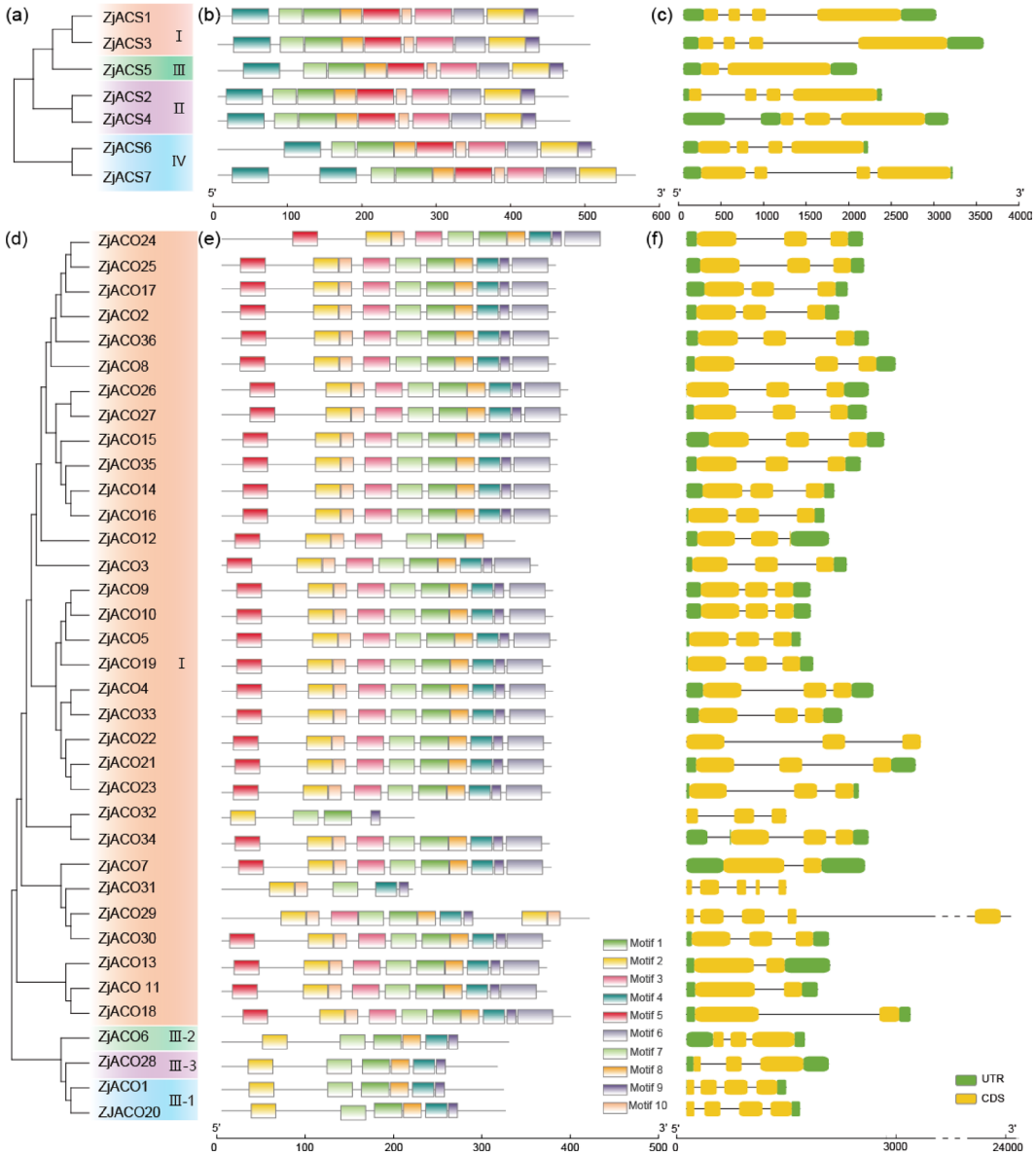

Fig. 4. The phylogenetic relationships, conserved motifs and gene structures of *ZjACSs* and *ZjACOs*. (**a**, **d**) The phylogenetic trees of *ZjACSs* and *ZjACOs* were built by MEGA11 utilizing the Neighbor-Joining (NJ) technique, incorporating 1000 bootstrap duplicates. Subtypes are distinguished by different colors. (**b**, **e**) Distribution of conserved motifs in *ZjACSs* and *ZjACOs*. Every enzyme family had 10 predicted motifs. (**c**, **f**) The gene structures of *ZjACSs* and *ZjACOs* included introns (illustrated by black lines), exons (depicted as yellow rectangles), and untranslated regions (UTRs, indicated by green rectangles).

ratio exceeding one, suggesting that they received strong and positive selection throughout the development of the 'Dongzao' ancestors. All the *Ka/Ks* ratios for the remaining duplicated gene pairs fell below one, suggesting that most might have undergone evolutionary purifying selection to preserve their structure.

To further illustrate the collinearity of the *ACS* and *ACO* genes and deduce their evolutionary links, we chose three representative species for comparison analysis with 'Dongzao', encompassing two jujube cultivars ('Suanzao' and 'Junzao') and *Arabidopsis thaliana* (Fig. 6b). A total of 11 *ZjACS* and 14 *ZjACO* genes exhibited collinear relationships with 'Suanzao' and 'Junzao', followed by Arabidopsis (12 *ZjACSs* and 8 *ZjACOs*) (Table S5). These findings revealed that the collinearity count between 'Junzao', 'Suanzao', and 'Dongzao' were higher than that between Arabidopsis and 'Dongzao'. Individual homologous genes exhibited either one-to-many or many-to-one homozygosity. Six *ACS* and three *ACO* genes (*ZjACS1*, *ZjACS2*, *ZjACS3*, *ZjACS5*, *ZjACS6*, *ZjACS7*, *ZjACO1*, *ZjACO6*, and *ZjACO20*) exhibited collinear relationships across all three chosen cultivars, indicating that these genes in the *ZjACS* and *ZjACO* gene families may have remained closely related throughout evolution.

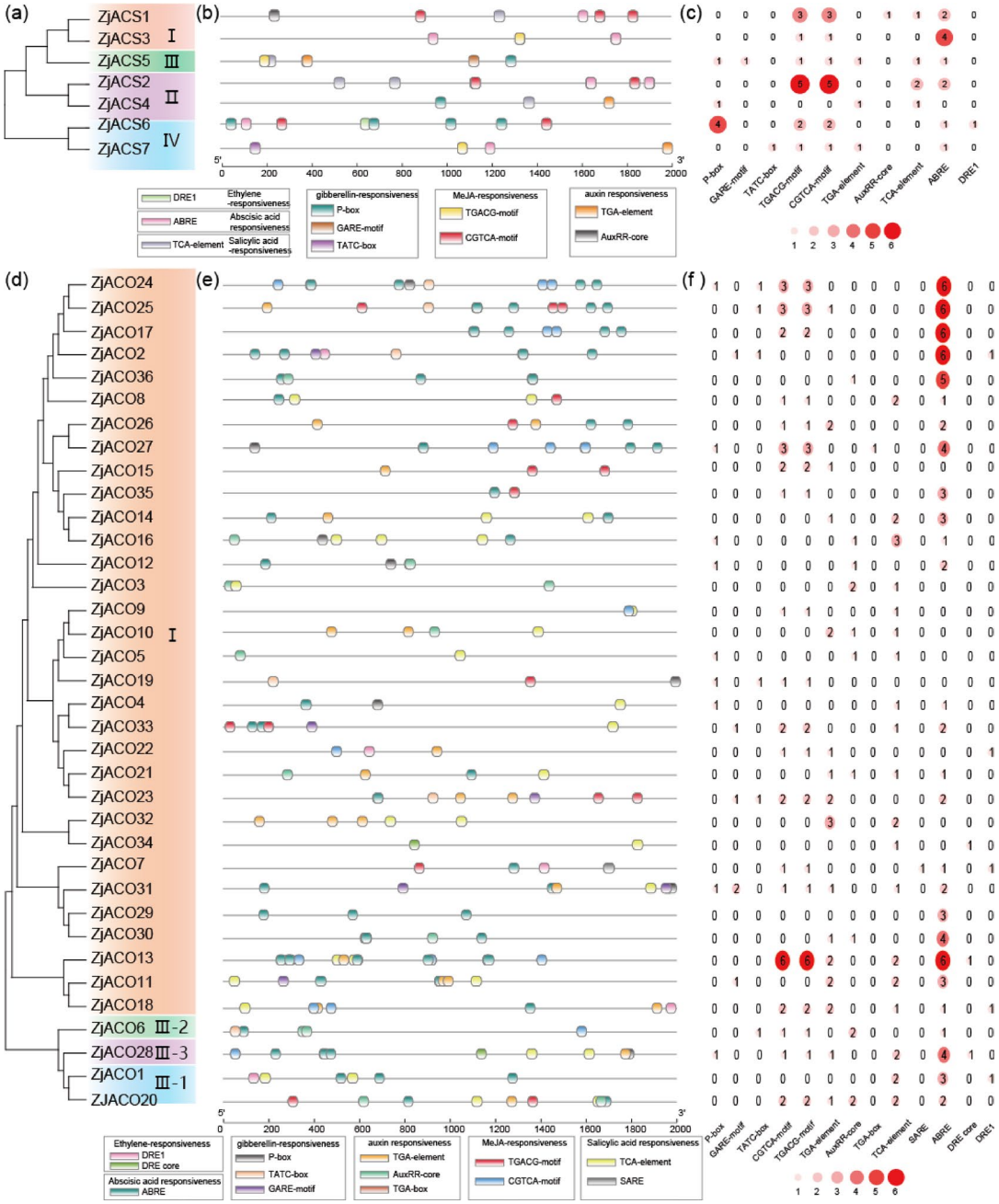

Fig. 5. Analysis of *cis*-elements in the promoters of the *ZjACS* and *ZjACO* genes. (**a**, **d**) The phylogenetic trees of ZjACS and ZjACO proteins were built by MEGA11 utilizing the Neighbor-Joining (NJ) method, with 1000 bootstrap replicates. Subtypes are distinguished by different colors. (**b**, **e**) Distribution of cis-acting elements identified in the 2000-bp promoter regions upstream of the *ZjACS* and *ZjACO* genes. (**c**, **f**) Heatmap of various *cis*-acting elements.

Expression profiles of *ZjACSs* and *ZjACOs* across different fruit developmental stages

To explore the possible functions of individual *ZjACS* and *ZjACO genes*, the expression patterns of the 7 *ZjACSs* and 36 *ZjACOs* across fruit growth were characterized using RNA-seq data (Fig. 7). Among the *ZjACS* genes (Fig. 7a), three *ZjACS* genes were up-regulated during fruit maturation processes, whereas others, such as *ZjACS6* and *ZjACS7*, were down-regulated. The expression of *ZjACS1* and *ZjACS5* peaked during the intermediate stage of fruit ripening. Among the *ZjACO* genes (Fig. 7b), 16 *ZjACOs* showed preferential expression during the later stages of fruit ripening, whereas *7 ZjACOs* were higher during the inital stages of fruit ripening. The remaining 13 genes showed little expression during fruit ripening. The higher *ACO* expression levels at later stages of fruit development may be conducive to fruit ripening.

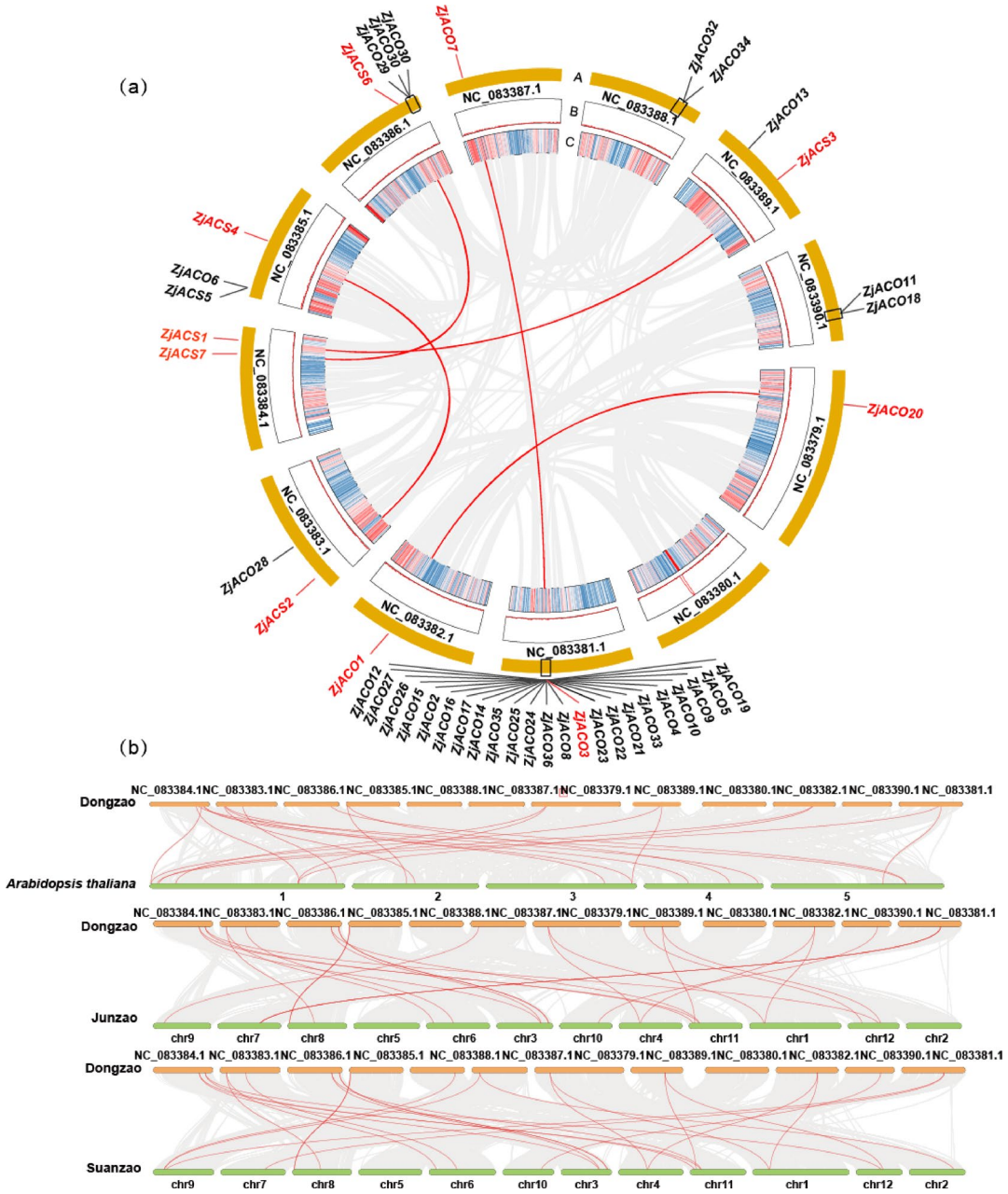

Fig. 6. Chromosome distribution and intraspecific interspecific collinearity analysis. (**a**) The distribution and collinearity of *ZjACS* and *ZjACO* genes on chromosomes. Black-marked genes do not exhibit collinearity, but red-marked genes do. Black rectangles that symbolize tandem repeat gene sets around tandem repeat genes. Circle A: The 12 chromosomes; B: gene density in liner plot; C: gene density in heatmap. (**b**) Synteny analysis of ACS and ACO genes of 'Dongzao' and 3 representative plants, namely. *Arabidopsis thaliana*, and jujube cultivars 'Junzao', and 'Suanzao'.

For confirming the reliability of the transcriptome data, the gene expression pattern of four *ZjACSs* and eight *ZjACOs* were chosen randomly for qRT-PCR analysis (Fig. 7c; Table S6). The results align with the transcriptome data, suggesting their credibility.

Co-expression of *ACS* and *ACO* genes and fruit ripening related transcription factors

Previous studies have revealed that members of the ERF[50], NAC[51], and WRKY[13] transcription factor families play important roles during fruit ripening. To further investigate the regulation of the *ZjACS* and *ZjACO* genes in 'Dongzao' jujube, co-expression networks for both the *ZjACS* and *ZjACO* genes were individually constructed. Firstly, we identified fruit ripening related transcription factors (ERF, NAC, and WRKY) in 'Dongzao' jujube from previous transcriptome data. Based on expression profiles, key TFs from the ERF family (15 in total), the NAC family (12), and the WRKY family (20) were selected, and the Pearson's correlation coefficients (PCs)

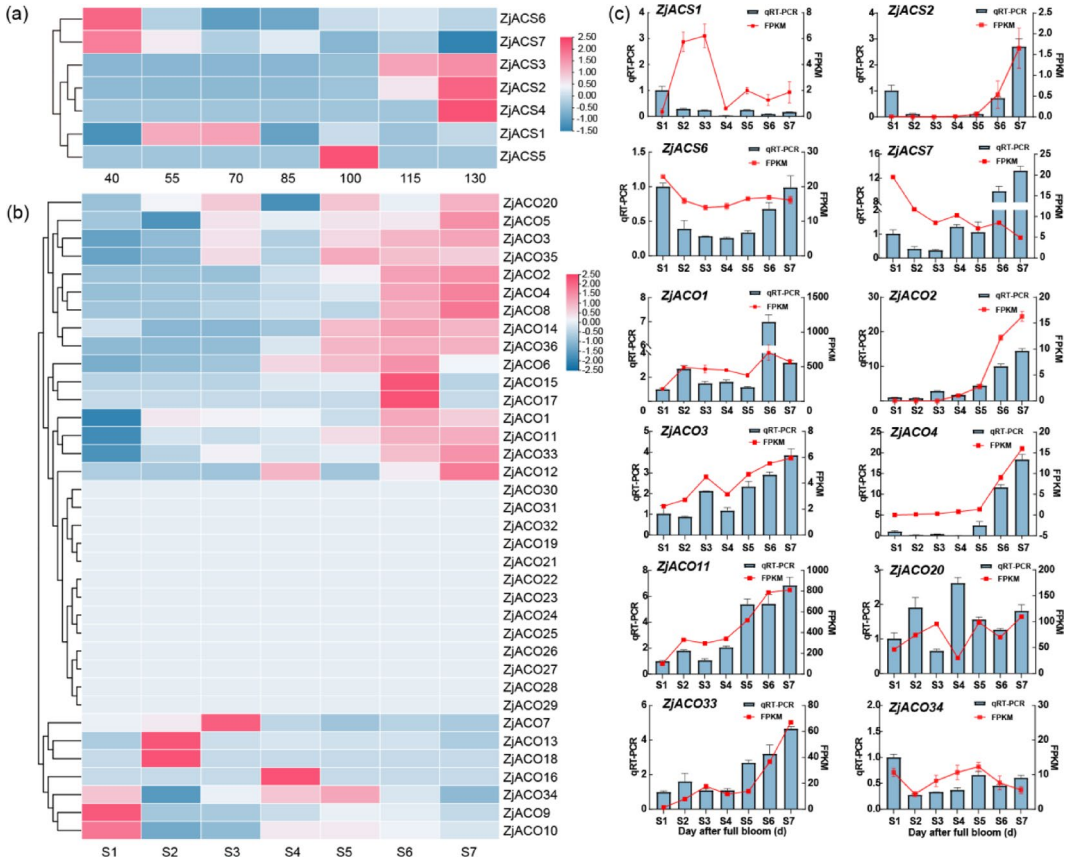

Fig. 7. Expression profiles and qRT-PCR expression analysis of *ZjACS* and *ZjACO* genes in cultivar 'Dongzao'. (**a**, **b**) Heatmap of the transcript levels of *ZjACS* (**a**) and *ZjACO* (**b**) genes. (**c**) Transcript levels of selected *ZjACS* and *ZjACO* genes in 'Dongzao' jujube fruit, sampled 40–130 days after full bloom (DAFB). Which gene was used as control and set to 0 or 1. 'qRT-PCR' is not really a unit for the y-axis – should have arbitrary units or set to 1 of some standards.

Fruit ripening related TFs	Number (percentage) of co-expressed *ZjACS* and *ZjACO* genes	
	ZjACSs	***ZjACOs***
ERF	4(57.14%)	7(19.44%)
NAC	2(28.57%)	8(22.22%)
WRKY	3(42.86%)	5(13.89%)

Table 1. The numbers of *ZjACS* and *ZjACO* genes co-expressed with fruit ripening-related TFs. Co expression analyses between the *ZjACS* and *ZjACO* genes and 15 ERF TFs, 12NAC TFs, and 20 WRKY TFs were conducted.

between these TFs and the 7 *ZjACS* genes and 36 *ZjACO* genes were calculated. After gene pairs with |PCs| < 0.9 were removed, the remaining gene pairs were used to build a co-expression network (Table S7). We identified 4 *ZjACS* genes, 9 *ZjACO* genes, 20 ERF TFs, 13 NAC TFs, and 12 WRKY TFs. Co-expression relationships were identified for 37 pairs between *ZjACS* genes and TFs and 128 pairs between *ZjACO* genes and TFs. More than 40% of these co-expressed *ZjACS* genes correlated with fruit ripening-related ERF and WRKY TFs, and 28.57% of *ZjACS* genes correlated with NAC TFs. For the *ZjACO* genes, about 20% of the *ZjACO* genes correlated with ERF and NAC TFs, and only 13.89% of the co-expressed *ZjACO* genes correlated with WRKY TFs (Table 1). Notably, *ZjERF2* had the most co-expression relationships and was highly correlated with 6 *ZjACOs*. Among them, *ZjACO2* had the highest correlation with *ZjERF2*.

Notes for Table 1. Co-expression analyses between the *ZjACS* and *ZjACO* genes and 15 ERF TFs, 12 NAC TFs, and 20 WRKY TFs were conducted.

Two networks were built to show the co-expression relationships between *ZjACSs*, *ZjACOs* genes and TFs involved in fruit ripening in the ERF, NAC, and WRKY families (Fig. 8). In the *ZjACSs* network, 31 TFs were

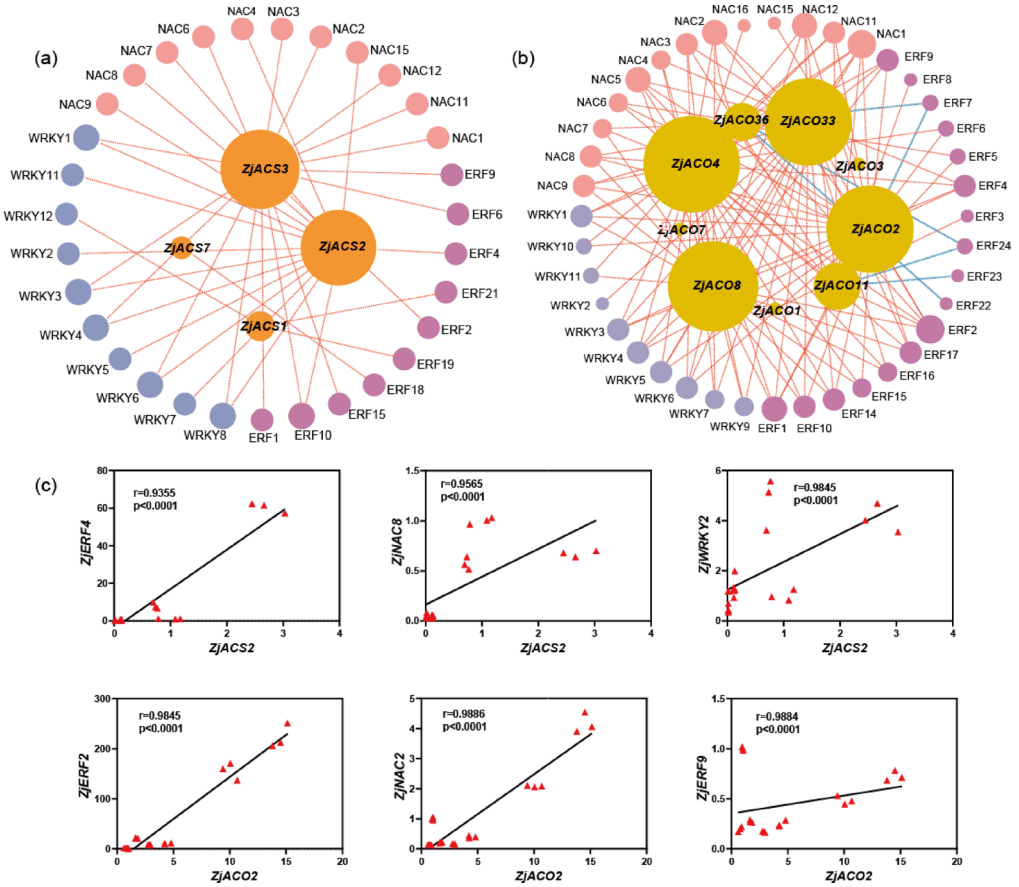

Fig. 8. Co-expression networks of fruit ripening related transcription factor families ERF, NAC, WRKY and ethylene synthesis related genes *ZjACSs* and *ZjACOs*. (**a**) Co-expression networks of *ZjACSs* and ERF, NAC, WRKY TFs using transcriptome data. (**b**) Co-expression networks of *ZjACOs* and ERF, NAC, WRKY TFs using transcriptome data. Reported fruit ripening related transcription factor families ERF, NAC, and WRKY were found in 'Dongzao' jujube and are denoted by various colored circle nodes, purple for ERF, pink for NAC, blue for WRKY. A red line connects two points, signifying a positive link ($0.9 \le r \le 1$) among the two genes, whereas a blue line depicts a negative link ($-0.9 \le r \le -1$) between the genes. The dimension of the nodes indicates the extent of relationships in co-expression. (**c**) Correlation of selected *ZjACSs*, and *ZjACOs* genes with ERF, NAC, and WRKY TFs using qRT-PCR data.

found to have positive correlations with *ZjACS* genes, including 10 ERF TFs, 11 NAC TFs, and 10 WRKY TFs. *ZjACS2* and *ZjACS3* exhibited extensive co-expression relationships. Specifically, the expression pattern of *ZjACS2* demonstrated the strongest correlation with *ZjWRKY2* (PC = 0.9845), while *ZjACS3* showed the highest correlation with *ZjWRKY1* (PC = 0.9679). In the *ZjACOs* network, the most commonly associated TFs belonged to the ERF family (17 TFs), followed by the NAC family (13 TFs) and then WRKY family (10 TFs). The majority of *ZjACO* genes displayed positive correlations with transcription factors, among which *ZjACO2/4/8/33* exhibited extensive co-expression relationships. *ZjACO2/4* is highly correlated with the expression of *ZjNAC2* (PC = 0.9886/ 0.9965). *ZjACO8/33* exhibited highly correlations with *ZjWRKY1* (PC = 0.9745) and *ZjERF10* (PC = 0.9834), respectively.

Discussion

ACS and ACO enzymes drive ethylene biosynthesis[18,52], with gene family expansions varing across species, such as Arabidopsis (12 *ACS* genes, 5 *ACO* genes)[18,30], pear (13 *ACS*, 11 *ACO*)[24], tomato (7 *ACS*, 11 *ACO*)[53] and watermelon (8 *ACS* and 8 *ACO*)[16]. In this study, a total of 7 *ZjACS* and an outstanding 36 *ZjACO* genes were identified within the genome of 'Dongzao' jujube. The numbers of *ZjACS* and *ZjACO* genes in 'Dongzao' jujube were about 0.6- and 3.3-folds of those in Arabidopsis, respectively, implying a lack of expansion of the *ACS* family and an obvious expansion of the *ACO* family in 'Dongzao' jujube. The variance observed is attributed to the evolutionary process and duplication in plants[49,54]. Consistent with the classification of the Arabidopsis *ACS* genes in previous studies[18,30], the 7 *ZjACS* genes in 'Dongzao' jujube were categorized into 4 types (type I, II, III, IV). While 36 *ZjACOs* formed four subgroups (type I, III-1, III-2, III-3) including a novel type I clade absent in model plants (Fig. 3). This specific expansion pattern reflected functional diversification through gene duplication events, particularly prominent in the *ACO* gene family.

The process of gene duplication plays a crucial part in the expansion of gene families and the formation of gene clusters through tandem duplication, whereas segmental duplications lead to the creation of similar genes, increasing the overall gene count and facilitating genetic drift[55]. In 'Dongzao' jujube, *ZjACS* genes exclusively arose from segmental duplication (7 genes), whereas *ZjACO* expansion primarily resulted from tandem duplication (30/36 genes) (Fig. 6). The *ZjACO* family was largely expanded in 'Dongzao' jujube when compared to Arabidopsis, which might be attributed to complex gene duplication of the *ZjACO* family that has not occurred in other lineages. Collinearity analysis identified 5 duplicated pairs (3 *ZjACSs*, 2 *ZjACOs*), with only *ZjACO20-ZjACO1* showing strong positive selection (*Ka/Ks* > 1), signifying a robust, favorable evolutionary selection of these genes. Cross-species comparisons revealed strongest synteny with 'Suanzao'/'Junzao' cultivars and weakest with *A. thaliana*, highlighting lineage-specific evolutionary paths. These patterns explain the *ACO* family's exceptional expansion in jujube compared to model plants, suggesting divergent selection pressures shaped ethylene biosynthesis genes during domestication[56].

The exon-intron structure and motif composition can be used to understand the evolutionary relationships among genes or organisms[57,58]. The exon–intron (Fig. 4) structure revealed that all 7 *ZjACS* and 36 *ZjACO* genes have introns. Introns ranged in number from 1 to 3 in *ZjACS* genes, and ranged from 2 to 4 in *ZjACO* genes. Notably, several *ZjACOs* genes (*ZjACO22*, *ZjACO29*, *ZjACO31*, and *ZjACO32*) lack untranslated regions (UTRs). This discrepancy may be associated with evolutionary gene loss and alternative splicing mechanisms[59–61]. Furthermore, previous studies have suggested that UTRs may play critical roles in transcriptional regulation[62,63]. In this study, the genes *ZjACO22*, *ZjACO29*, *ZjACO31*, and *ZjACO32*, which lack UTRs, exhibited low expression level (Fig. 7). It is speculated that their transcription might be impaired, although specific roles remain to be elucidated through further research. Motif analysis (Fig. 4) showed that motif 9 in the predicted ZjACS proteins was common in all except the type IV gene encoding ZjACS7. Among the ZjACO proteins, motif 5 was present only in proteins encoded by type I genes. Typically, closely related gene members exhibit comparable structural traits, as seen in plants like Arabidopsis[64], and sand pear[30], indicating that these structures are evolutionarily preserved. These structural studies provided independent support for the phylogeny and categorization conclusions.

The promoters of genes contain diverse *cis*-elements that mediate the accurate binding of effector proteins to template DNA, which either activates or impedes gene transcription. Consequently, gene function can be deduced through the identification of *cis*-elements[65]. Plant hormones have been shown to regulate gene expression in several plants[66]. Promoter analysis of *ZjACS* and *ZjACO* genes revealed abundant hormone-responsive cis-elements (ABA, MeJA, GA, SA, auxin and ethylene) (Fig. 5), indicating their integration into phytohormone signaling networks. Notably, *ZjACS2* and *ZjACO13* included many MeJA-responsive elements, suggesting that *ZjACS2* and *ZjACO13* may be induced by MeJA or abiotic stress. Moreover, the *ZjACO2* and *ZjACO11* promoters contained ethylene-responsive elements, and these genes exhibited higher expression in later stages of fruit ripening. The *ZjACS6* promoter also contained ethylene-responsive elements, and exhibited a higher expression during the initial phases of fruit ripening. Together, these results suggested that transcriptional regulation of ethylene biosynthesis genes through hormonal cross-talk, particularly through ABA and ethylene signals.

To analyse the roles of *ZjACS* and *ZjACO* genes in 'Dongzao' jujube during ripening, we profiled their expression patterns throughout the growth and maturation phases of the fruit (Fig. 7). Over 60% of the *ZjACS* and *ZjACO* genes were expressed differently throughout fruit growth and ripening, suggesting significant influence of the *ACS* and *ACO* families in regulating ethylene-mediated fruit ripening in 'Dongzao'. The expression levels of genes controlling ethylene biosynthesis (*ZjACS2*, *ZjACO2/4/8/11/33*) remained low at the early maturation stage in 'Dongzao' jujube, but increased significantly at the half-red and full-red stages. This expression pattern aligned with the elevated ethylene production during fruit ripening reported by Zhang et al.[67] in 'Dongzao' jujube, suggesting that these genes may respond to the increase in endogenous ethylene emission. In non-climacteric blueberry fruits, the expression of *ACS1* was up-regulated, preceding the ethylene increase. *ACO2* transcript level increased significantly during later maturation stages, indicating that both *ACS1* and *ACO2* mediate ethylene accumulation to participate in fruit maturation[68]. Notably, type IV ACS-like genes, which are derived from the AATase gene were prominent[64]. In Arabidopsis, *AtACS10* and *AtACS12* are assumed to be amino acid transferases without ACS activity[64]. However, Zhang et al.[30] have reported that, while low, the expression of *PpyACS12* and *PpyACS13* were constitutive during sand pear development. Thus, ACS-like gene expression patterns in sand pear indicate that ACS-like genes might have functions in the biosynthesis of ethylene. In our study, the type IV *ZjACS6* and *ZjACS7* exhibited obvious opposite expression trends during fruit ripening. Therefore, we also speculated that these two genes might play a role in ethylene biosynthesis and were negatively correlated with fruit ripening.

Co-expression analyses (Fig. 8) showed that *ZjACS* and *ZjACO* genes were tightly co-expressed with known fruit ripening-related TFs (ERF, NAC, and WRKY). Among them, *ZjACS3-ZjWRKY1*, *ZjACO2-ZjNAC2/ZjERF2*, *ZjACO4-ZjNAC2*, *ZjACO8-ZjWRKY1*, and *ZjACO33-ZjERF10* exhibited highly correlations. It suggested a coordinated regulatory module governing ethylene biosynthesis during 'Dongzao' jujube ripening. In kiwifruit, *AdACSs* and *AdACOs* were regulated by ERF and NAC TFs to amplified ethylene biosynthesis[69]. The similar relationships (*ZjACS3/ZjACO8-ZjWRKY1*, *ZjACO2/4-ZNAC2*) in 'Dongzao' jujube, implies that ethylene signaling may operate through conserved transcriptional hubs. In banana, *MaERF11* regulated the expression of *MaEXP2*/7/8 and *MaACO1* by binding to the GCC-box motif within their promoter regions[70]. Wei et al.[71] reported that the NAC TF MaNAC083 affected fruit ripening by inhibiting the transcription of five ethylene biosynthesis genes (*MaACS1* and *MaACO1/4/5/8*). In *Arabidopsis thaliana*, AtWRKY29 positively regulated the expression of *AtACS5/6/8/11* and *AtACO5* and promoted ethylene biosynthesis in roots[72]. Among the co-expression network, ZjERF2/10, ZjNAC2 and ZjWRKY1 were candidate TFs for regulation of ethylene biosynthesis, and it was speculated that they played a similar regulatory role in 'Dongzao' jujube. The specific

regulatory mechanisms require further experimental validation, and the following approaches could be used in subsequent studies: (1) investigating the regulatory effects of target genes on ethylene biosynthesis through virus-induced gene silencing (VIGS) or transient over-expression; (2) characterizing transcription factor interactions with putative target genes using dual-luciferase reporter assays or electrophoretic mobility shift assays (EMSA); (3) given the limitations of the jujube genetic transformation system, assessing functional conservation via heterologous expression in model plant systems.

Conclusion

In this study, we provide a systemic analysis on the *ACS* and *ACO* genes of 'Dongzao' jujube. A total of 7 *ZjACS* and 36 *ZjACO* genes were identified and characterized. Furthermore, phylogenetic relationships, chromosomal distribution, duplication events, conserved motifs, promoter region *cis*-regulatory elements and expression levels during different fruit developmental stages were all investigated. These analyses helped to classify these genes and provide insights into the evolution of the *ACS* and *ACO* gene families. The expression pattern of the *ZjACSs* and *ZjACOs* may provide a preliminary knowledge of their function during fruit ripening. Moreover, we predicted key *ZjACSs*, *ZjACOs* and related TFs that may play roled in fruit ripening through co-expression analysis. Their functions will be investigated in further studies to better understand the regulation of fruit ripening in 'Dongzao' jujube. Together, this extensive genomic examination of *ACS* and *ACO* genes in 'Dongzao' jujube provides new perspectives for upcoming functional analyses of fruit maturation.

Data availability

Genome data have been deposited at NCBI and are publicly available (ASM3175591v1). RNA-seq data used in this work were deposited at NCBI and are publicly available (SRA: PRJNA1173509).

Received: 5 January 2025; Accepted: 19 May 2025
Published online: 24 May 2025

References

1. Zhao, H., Yin, C. C., Ma, B., Chen, S. Y. & Zhang, J. S. Ethylene signaling in rice and *Arabidopsis*: New regulators and mechanisms. *J. Integr. Plant. Biol.* **63**, 102–125. https://doi.org/10.1111/jipb.13028 (2021).
2. Li, D. et al. Ethylene-independent functions of the ethylene precursor ACC in *Marchantia polymorpha*. *Nat. Plants*. **6**, 1335–1344. https://doi.org/10.1038/s41477-020-00784-y (2020).
3. Li, X. et al. The cotton *GhWIN2* gene activates the cuticle biosynthesis pathway and influences the salicylic and jasmonic acid biosynthesis pathways. *BMC Plant. Biol.* **19**, 379. https://doi.org/10.1186/s12870-019-1888-6 (2019).
4. Hughes, P. W. OsGSK2 integrates jasmonic acid and brassinosteroid signaling in rice. *Plant. Cell.* **32**, 2669–2670. https://doi.org/10.1105/tpc.20.00531 (2020).
5. Wybouw, B. & De Rybel, B. Cytokinin—a developing story. *Trends Plant. Sci.* **24**, 177–185. https://doi.org/10.1016/j.tplants.2018.10.012 (2019).
6. Zhang, S. et al. Expression of cotton PLATZ1 in transgenic *Arabidopsis* reduces sensitivity to osmotic and salt stress for germination and seedling establishment associated with modification of the abscisic acid, Gibberellin, and ethylene signalling pathways. *BMC Plant. Biol.* **18**, 218. https://doi.org/10.1186/s12870-018-1416-0 (2018).
7. Brookbank, B. P., Patel, J., Gazzarrini, S. & Nambara, E. Role of basal ABA in plant growth and development. *Genes (Basel)* **12**. https://doi.org/10.3390/genes12121936 (2021).
8. Chen, K. et al. Abscisic acid dynamics, signaling, and functions in plants. *J. Integr. Plant. Biol.* **62**, 25–54. https://doi.org/10.1111/jipb.12899 (2020).
9. Planas-Riverola, A. et al. Brassinosteroid signaling in plant development and adaptation to stress. *Development* **146** https://doi.org/10.1242/dev.151894 (2019).
10. Van de Poel, B., Smet, D. & Van Der Straeten, D. Ethylene and hormonal cross talk in vegetative growth and development. *Plant. Physiol.* **169**, 61–72. https://doi.org/10.1104/pp.15.00724 (2015).
11. Li, S., Chen, K. & Grierson, D. A critical evaluation of the role of ethylene and MADS transcription factors in the network controlling fleshy fruit ripening. *New. Phytol.* **221**, 1724–1741. https://doi.org/10.1111/nph.15545 (2019).
12. Dubois, M., Van den Broeck, L. & Inzé, D. The pivotal role of ethylene in plant growth. *Trends Plant. Sci.* **23**, 311–323. https://doi.org/10.1016/j.tplants.2018.01.003 (2018).
13. Liu, M. et al. Ethylene biosynthesis and signal transduction during ripening and softening in non-climacteric fruits: An overview. *Front. Plant. Sci.* **15**, 1368692. https://doi.org/10.3389/fpls.2024.1368692 (2024).
14. Paul, V., Pandey, R. & Srivastava, G. C. The fading distinctions between classical patterns of ripening in climacteric and non-climacteric fruit and the ubiquity of ethylene—an overview. *J. Food Sci. Technol.* **49**, 1–21. https://doi.org/10.1007/s13197-011-0293-4 (2012).
15. Fenn, M. A. & Giovannoni, J. J. Phytohormones in fruit development and maturation. *Plant. J.* **105**, 446–458. https://doi.org/10.1111/tpj.15112 (2021).
16. Zhou, M. et al. Comparative dynamics of ethylene production and expression of the *ACS* and *ACO* genes in normal-ripening and non-ripening watermelon fruits. *Acta Physiol. Plant.* **38**, 228. https://doi.org/10.1007/s11738-016-2248-x (2016).
17. Ma, W. et al. Melatonin alters the secondary metabolite profile of grape berry skin by promoting *VvMYB14*-mediated ethylene biosynthesis. *Hortic. Res.* **8**, 43. https://doi.org/10.1038/s41438-021-00478-2 (2021).
18. Pattyn, J., Vaughan-Hirsch, J. & Van de Poel, B. The regulation of ethylene biosynthesis: A complex multilevel control circuitry. *New. Phytol.* **229**, 770–782. https://doi.org/10.1111/nph.16873 (2021).
19. Khan, S., Alvi, A. F., Saify, S., Iqbal, N. & Khan, N. A. The ethylene biosynthetic enzymes, 1-aminocyclopropane-1-carboxylate (ACC) synthase (ACS) and ACC oxidase (ACO): The less explored players in abiotic stress tolerance. *Biomolecules* **14** https://doi.org/10.3390/biom14010090 (2024).
20. Yin, L. et al. Genome-wide identification and expression analysis of 1-aminocyclopropane-1-carboxylate synthase (*ACS*) gene family in *Chenopodium quinoa*. *Plants-Basel* **12**. https://doi.org/10.3390/plants12234021 (2023).
21. Houben, M. & Van de Poel, B. 1-Aminocyclopropane-1-Carboxylic acid oxidase (ACO): the enzyme that makes the plant hormone ethylene. *Front. Plant. Sci.* **10** https://doi.org/10.3389/fpls.2019.00695 (2019).
22. Liu, M., Pirrello, J., Chervin, C., Roustan, J. P. & Bouzayen, M. Ethylene control of fruit ripening: Revisiting the complex network of transcriptional regulation. *Plant. Physiol.* **169**, 2380–2390. https://doi.org/10.1104/pp.15.01361 (2015).
23. Mu, Q. et al. Comparison and verification of the genes involved in ethylene biosynthesis and signaling in apple, grape, peach, pear and strawberry. *Acta Physiol. Plant.* **38** https://doi.org/10.1007/s11738-016-2067-0 (2016).

24. Yuan, H., Yue, P., Bu, H., Han, D. & Wang, A. Genome-wide analysis of *ACO* and *ACS* genes in Pear (*Pyrus ussuriensis*). *Vitro Cell. Dev. Biol. Plant.* **56**, 193–199. https://doi.org/10.1007/s11627-019-10009-3 (2020).
25. Li, T. et al. Apple (*Malus domestica*) MdERF2 negatively affects ethylene biosynthesis during fruit ripening by suppressing *MdACS1* transcription. *Plant. J.* **88**, 735–748. https://doi.org/10.1111/tpj.13289 (2016).
26. Li, T. et al. Comparative transcriptome analysis of the climacteric of apple fruit uncovers the involvement of transcription factors affecting ethylene biosynthesis. *Hortic. Plant. J.* **9**, 659–669. https://doi.org/10.1016/j.hpj.2022.12.002 (2023).
27. Kou, X., Liu, C., Han, L., Wang, S. & Xue, Z. NAC transcription factors play an important role in ethylene biosynthesis, reception and signaling of tomato fruit ripening. *Mol. Genet. Genomics* **291**, 1205–1217. https://doi.org/10.1007/s00438-016-1177-0 (2016).
28. Gan, Z. et al. AcWRKY40 mediates ethylene biosynthesis during postharvest ripening in kiwifruit. *Plant. Sci.* **309** https://doi.org/10.1016/j.plantsci.2021.110948 (2021).
29. Upadhyay, R. K. et al. Comprehensive profiling of endogenous phytohormones and expression analysis of 1-aminocyclopropane-1-carboxylic acid synthase gene family during fruit development and ripening in octoploid strawberry (*Fragaria× ananassa*). *Plant. Physiol. Biochem.* **196**, 186–196. https://doi.org/10.1016/j.plaphy.2023.01.031 (2023).
30. Zhang, J. G. et al. Genome-wide identification of the 1-Aminocyclopropane-1-carboxylic acid synthase (*ACS*) genes and their possible role in sand Pear (*Pyrus pyrifolia*) fruit ripening. *Horticulturae* **7**. https://doi.org/10.3390/horticulturae7100401 (2021).
31. Munoz-Robredo, P. et al. Study on differential expression of 1-aminocyclopropane-1-carboxylic acid oxidase genes in table grape Cv. Thompson seedless. *Postharvest Biol. Technol.* **76**, 163–169. https://doi.org/10.1016/j.postharvbio.2012.10.006 (2013).
32. Zhang, S. et al. The transcriptional regulatory mechanisms exploration of jujube biological traits through multi-omics analysis. *Forests* **15** https://doi.org/10.3390/f15020395 (2024).
33. Zhang, Q. et al. Transcriptome and metabolome profiling unveil the mechanisms of *Ziziphus jujuba* mill. Peel coloration. *Food Chem.* **312** https://doi.org/10.1016/j.foodchem.2019.125903 (2020).
34. Zhu, Z., Zhang, Z., Qin, G. & Tian, S. Effects of brassinosteroids on postharvest disease and senescence of jujube fruit in storage. *Postharvest Biol. Technol.* **56**, 50–55. https://doi.org/10.1016/j.postharvbio.2009.11.014 (2010).
35. Li, K. et al. Haplotype-resolved T2T reference genomes for wild and domesticated accessions shed new insights into the domestication of jujube. *Hortic. Res.* **11**, uhae071. https://doi.org/10.1093/hr/uhae071 (2024).
36. El-Gebali, S. et al. The Pfam protein families database in 2019. *Nucleic Acids Res.* **47**, D427–d432. https://doi.org/10.1093/nar/gky995 (2019).
37. Hu, B. et al. GSDS 2.0: An upgraded gene feature visualization server. *Bioinformatics* **31**, 1296–1297. https://doi.org/10.1093/bioinformatics/btu817 (2015).
38. Bailey, T. L. et al. MEME SUITE: Tools for motif discovery and searching. *Nucleic Acids Res.* **37**, W202–208. https://doi.org/10.1093/nar/gkp335 (2009).
39. Shu, Y., Liu, Y., Zhang, J., Song, L. & Guo, C. Genome-wide analysis of the AP2/ERF superfamily genes and their responses to abiotic stress in *Medicago truncatula*. *Front. Plant. Sci.* **6**, 1247. https://doi.org/10.3389/fpls.2015.01247 (2015).
40. Lescot, M. et al. PlantCARE, a database of plant *cis*-acting regulatory elements and a portal to tools for in silico analysis of promoter sequences. *Nucleic Acids Res.* **30**, 325–327. https://doi.org/10.1093/nar/30.1.325 (2002).
41. Chen, C. et al. TBtools: An integrative toolkit developed for interactive analyses of big biological data. *Mol. Plant.* **13**, 1194–1202. https://doi.org/10.1016/j.molp.2020.06.009 (2020).
42. Wang, Y. et al. MCScanX: A toolkit for detection and evolutionary analysis of gene synteny and collinearity. *Nucleic Acids Res.* **40**, e49. https://doi.org/10.1093/nar/gkr1293 (2012).
43. Zhang, Z. KaKs_Calculator 3.0: Calculating selective pressure on coding and non-coding sequences. *Genomics Proteom. Bioinf.* **20**, 536–540. https://doi.org/10.1016/j.gpb.2021.12.002 (2022).
44. Kim, D., Langmead, B. & Salzberg, S. L. HISAT: A fast spliced aligner with low memory requirements. *Nat. Methods* **12**, 357–360. https://doi.org/10.1038/nmeth.3317 (2015).
45. Anders, S. & Huber, W. Differential expression analysis for sequence count data. *Genome Biol.* **11**(R106). https://doi.org/10.1186/gb-2010-11-10-r106(2010).
46. Shannon, P. et al. Cytoscape: A software environment for integrated models of biomolecular interaction networks. *Genome Res.* **13**, 2498–2504. https://doi.org/10.1101/gr.1239303 (2003).
47. Livak, K. J. & Schmittgen, T. D. Analysis of relative gene expression data using real-time quantitative PCR and the 2(-Delta Delta C(T)) method. *Methods* **25**, 402–408. https://doi.org/10.1006/meth.2001.1262 (2001).
48. Seymour, G. B., Østergaard, L., Chapman, N. H., Knapp, S. & Martin, C. Fruit development and ripening. *Annu. Rev. Plant. Biol.* **64**, 219–241. https://doi.org/10.1146/annurev-arplant-050312-120057 (2013).
49. Liang, J. et al. Comprehensive characterization and expression analysis of enzymatic antioxidant gene families in passion fruit (*Passiflora edulis*). *iScience* **26** https://doi.org/10.1016/j.isci.2023.108329 (2023).
50. Sun, Q. et al. The abscisic acid-responsive transcriptional regulatory module CsERF110-CsERF53 orchestrates citrus fruit coloration. *Plant. Commun.* **5**, 101065. https://doi.org/10.1016/j.xplc.2024.101065 (2024).
51. Wu, Y. Y. et al. Methyl jasmonate enhances ethylene synthesis in kiwifruit by inducing *NAC* genes that activate *ACS1*. *J. Agric. Food Chem.* **68**, 3267–3276. https://doi.org/10.1021/acs.jafc.9b07379 (2020).
52. Xu, C. et al. Dual activities of ACC synthase: novel clues regarding the molecular evolution of *ACS* genes. *Sci. Adv.* **7**. https://doi.org/10.1126/sciadv.abg8752 (2021).
53. Ding, Q. et al. Identification and expression analysis of hormone biosynthetic and metabolism genes in the 2OGD family for identifying genes that May be involved in tomato fruit ripening. *Int. J. Mol. Sci.* **21**. https://doi.org/10.3390/ijms21155344 (2020).
54. Sun, R., Wang, S., Ma, D., Li, Y. & Liu, C. Genome-wide analysis of cotton auxin early response gene families and their roles in somatic embryogenesis. *Genes* **10**. https://doi.org/10.3390/genes10100730 (2019).
55. Zhang, Z. & Li, X. Genome-wide identification of *AP2/ERF* superfamily genes and their expression during fruit ripening of Chinese jujube. *Sci. Rep.* **8**. https://doi.org/10.1038/s41598-018-33744-w (2018).
56. Xie, T. et al. Genome-wide investigation of WRKY gene family in pineapple: evolution and expression profiles during development and stress. *BMC Genom.* **19**. https://doi.org/10.1186/s12864-018-4880-x (2018).
57. Bondarenko, V. S. & Gelfand, M. S. Evolution of the exon-intron structure in ciliate genomes. *PloS One* **11**. https://doi.org/10.1371/journal.pone.0161476 (2016).
58. Poverennaya, I. V. & Roytberg, M. A. Spliceosomal introns: Features, functions, and evolution. *Biochemistry (Mosc)* **85**, 725–734. https://doi.org/10.1134/s0006297920070019 (2020).
59. Lurin, C. et al. Genome-wide analysis of Arabidopsis pentatricopeptide repeat proteins reveals their essential role in organelle biogenesis. *Plant. Cell.* **16**, 2089–2103. https://doi.org/10.1105/tpc.104.022236 (2004).
60. Peng, Q. S., Lu, M. D., Yang, M. Q., Li, J. W. & Yue, Y. L. Bioinformatic analysis of PPR gene family in soybean. *Soybean Sci.* **40**, 177–185. https://doi.org/10.11861/j.issn.1000-9841.2021.02.0177 (2021).
61. Han, Y. H., Chen, Q., Zhang, H., Wang, H. M. & Chen, Q. J. Bioinformatics analysis of invertase gene family in cotton. *J. China Agric. Univ.* **23**, 15–30. https://doi.org/10.11841/j.issn.1007-4333.2018.11.02 (2018).
62. Xu, R., Ye, X. & Quinn Li, Q. AtCPSF73-II gene encoding an Arabidopsis homolog of CPSF 73 kda subunit is critical for early embryo development. *Gene* **324**, 35–45. https://doi.org/10.1016/j.gene.2003.09.025 (2004).
63. Bruhn, O. et al. Length variants of the ABCB1 3'-UTR and loss of MiRNA binding sites: possible consequences in regulation and pharmacotherapy resistance. *Pharmacogenomics* **17**, 327–340. https://doi.org/10.2217/pgs.15.175 (2016).

64. Zhang, T. C., Qiao, Q. & Zhong, Y. Detecting adaptive evolution and functional divergence in aminocyclopropane-1-carboxylate synthase (ACS) gene family. *Comput. Biol. Chem.* **38**, 10–16. https://doi.org/10.1016/j.compbiolchem.2012.04.001 (2012).
65. Li, Y. et al. Genome-wide identification and expression analysis of NAC family genes in *Ginkgo biloba* L. *Plant. Biol. (Stuttg).* **25**, 107–118. https://doi.org/10.1111/plb.13486 (2023).
66. Wang, J. Y., Wang, J. P. & Yang, H. F. Identification and functional characterization of the NAC gene promoter from *Populus euphratica*. *Planta* **244**, 417–427. https://doi.org/10.1007/s00425-016-2511-9 (2016).
67. Zhang, Z., Huang, J. & Li, X. Transcript analyses of ethylene pathway genes during ripening of Chinese jujube fruit. *J. Plant. Physiol.* **224–225**, 1–10. https://doi.org/10.1016/j.jplph.2018.03.004 (2018).
68. Wang, Y. W. et al. Atypical climacteric and functional ethylene metabolism and signaling during fruit ripening in blueberry (*Vaccinium* sp). *Front. Plant. Sci.* **13**, 932642. https://doi.org/10.3389/fpls.2022.932642 (2022).
69. Wang, J. et al. Transcriptional and post-transcriptional regulation of ethylene biosynthesis by exogenous acetylsalicylic acid in Kiwifruit. *Hortic. Res.* **9**. https://doi.org/10.1093/hr/uhac116 (2022).
70. Han, Y. C. et al. Banana transcription factor MaERF11 recruits histone deacetylase MaHDA1 and represses the expression of MaACO1 and expansins during fruit ripening. *Plant. Physiol.* **171**, 1070–1084. https://doi.org/10.1104/pp.16.00301 (2016).
71. Wei, W. et al. MaMADS1-MaNAC083 transcriptional regulatory cascade regulates ethylene biosynthesis during banana fruit ripening. *Hortic. Res.* **10**, uhad177. https://doi.org/10.1093/hr/uhad177 (2023).
72. Wang, Z. et al. WRKY29 transcription factor regulates ethylene biosynthesis and response in arabidopsis. *Plant Physiol. Biochem.* **194**, 134–145. https://doi.org/10.1016/j.plaphy.2022.11.012 (2023).

Acknowledgements

This work was supported by National Key R&D Program of China (2024YFD2200600), Henan Science and Technology Research and Development Project (252102111159) and the National Project of Improved Forestry Varieties Cultivation. We are grateful to Anita K. Snyder for critical reading and editing the paper.

Author contributions

Investigation, formal analysis, visualization, methodology, Z.C., Z.Z., and G.J.; writing - original draft, Z.C., G.J. and S.Z.; data curation, Y.G. and Y.L.; funding acquisition, G.-P.Z. and M.Z.; conceptualization, writing - review & editing, Z.Z, M.Z and S.Z.; supervision, project administration, Z.Z., M.Z. and S. Z.; All authors have read and agreed to the published version of the manuscript.

Declarations

Competing interests

The authors declare no competing interests.

Additional information

Correspondence and requests for materials should be addressed to G.-P.Z., M.Z. or S.Z.

Reprints and permissions information is available at www.nature.com/reprints.

Publisher's note Springer Nature remains neutral with regard to jurisdictional claims in published maps and institutional affiliations.